ELSEVIER

Journal of Nuclear Materials 266–269 (1999) 251–257

journal of nuclear materials

Stability of the detachment front in a tokamak divertor

S.I. Krasheninnikov [a,*], M. Rensink [b], T.D. Rognlien [b], A.S. Kukushkin [c,d], J.A. Goetz [a], B. LaBombard [a], B. Lipschultz [a], J.L. Terry [a], M. Umansky [a]

[a] *Massachusetts Institute of Technology, Plasma Science and Fusion Center, 167 Albany Street, Room NW 16-234, 77 Massachusetts Ave, Cambridge, MA 02139, USA*

[b] *Lawrence Livermore National Laboratory, Livermore, CA 94550, USA*

[c] *ITER Garching Joint Work Site, Max-Planck-Institut für Plasmaphysik, Boltzmannstraße 2, D-85748 Garching bei München, Germany*

[d] *I. V. Kurchatov Institute of Atomic Energy, 1 Kurchatov Sq., Moscow 123098, Russia*

Abstract

Experimental observations show that when a divertor plasma detaches, radiation regions (fronts) move towards the X-point. This indicates that the localization of the fronts in the divertor is unstable. We study theoretically the stability of detached divertor operation and compare our results with experimental data. We show that the impurity radiation and plasma recombination effects play a crucial role in the evolution of detached plasma parameters. In the tokamak SOL these effects result in the saturation of upstream plasma density and temperature as the total number of particles (ions and neutrals) in the SOL is increased, and cause both impurity radiation and ionization–recombination fronts propagation towards the X-point. These conclusions are supported by experimental data from Alcator C-Mod.

Keywords: Tokamak; Detachment; Stability; Impurity; Recombination

1. Introduction

Experimental observations show that impurity and hydrogen radiation regions in divertor plasmas move towards the X-point as detachment proceeds [1,2]. Such motion of the radiation regions is also seen in two dimensional (2D) modeling of the scrape-off-layer (SOL) plasmas [3–5] although the physics of these effects was not studied in detail.

Even though this shift of the radiation regions may be not crucial for the performance of divertor itself, it can be a cause for important experimental observations during detachment; e.g., core plasma confinement degradation and enhancement of neutral gas pressure in main chamber arising from increased neutral gas leakage from the divertor region.

This paper presents a theoretical study of the stability of detached divertor operation and comparison with experimental data. The paper is organized as follows: in Section 2, we discuss the physics of detached divertor operation instabilities driven by energy loss due to impurity and hydrogen radiation; in Section 3, the variation of divertor plasma parameters caused by these instabilities is illustrated with 2D modeling results; in Section 4, we compare our theoretical findings with experimental data from Alcator C-Mod; and in Section 5, we summarize the main conclusions.

2. Mechanisms of detached divertor operation instabilities

In low temperature divertor plasmas, impurity radiation mainly occurs in regions, where the electron temperature $T \sim 10$ eV and higher, hydrogen ionization occurs near $T \sim 5$ eV, and plasma recombination near $T \sim 1$ eV and lower. We will refer to these regions as fronts even though they can be quite extended in space (e.g. plasma volumetric recombination region). Differences in the temperatures associated with these fronts result in different locations of the fronts in divertor

* Corresponding author. Tel.: +1-617 253 0478; fax: +1-617 253 0448; e-mail: krash@psfc.mit.edu.

0022-3115/99/$ – see front matter
PII: S0022-3115(98)00577-7

volume (Fig. 1). Therefore, in our simplified analytic analysis in this section, we will treat each front separately and account for their interactions as boundary conditions.

The regimes of the SOL plasmas we are interested in are so-called high recycling regimes. In such regimes plasma flux from the core into the divertor volume is much smaller than the plasma source in the divertor caused by ionization of neutral gas (plasma recycling). The neutral gas is originated by plasma neutralization at material surfaces or volumetric recombination. To sustain the SOL plasma by recycling processes in the divertor, it is necessary to have power input to the plasma recycling region, Q_H, since the ionization of each hydrogenic neutral particle 'costs' $E_{ion} \gtrsim 30$ eV due to hydrogen radiation. Therefore, high recycling regimes can be sensitive to the energy balance.

Due to the spatial separation of the fronts caused by the temperature dependence of different atomic processes, power balance in the SOL (involving the power coming into the SOL from the core, Q_{SOL}, impurity radiation loss in the SOL, $Q_{rad}^{(imp)}$, and Q_H) can be written as $Q_H = Q_{SOL} - Q_{rad}^{(imp)}$. We will see that the effects of impurity radiation and plasma recombination impose restrictions on the power sources, Q_{SOL} and Q_H, which are needed to sustain a high recycling SOL plasma at a given upstream plasma pressure, P_{up}. Both Q_{SOL} and Q_H must exceed critical values which depend on P_{up}, $Q_{SOL} > \hat{Q}_{imp}(P_{up})$ and $Q_H > \hat{Q}_{rec}(P_{up})$, and associated, respectively, with impurity radiation and plasma recombination. Of course, in experiments, the effects of impurity radiation and plasma recombination in the recycling region may be strongly coupled. However, to emphasize the differences in the physics of these instabilities, our theoretical model can treat them separately by, for example, turning off the impurity or plasma recombination effects.

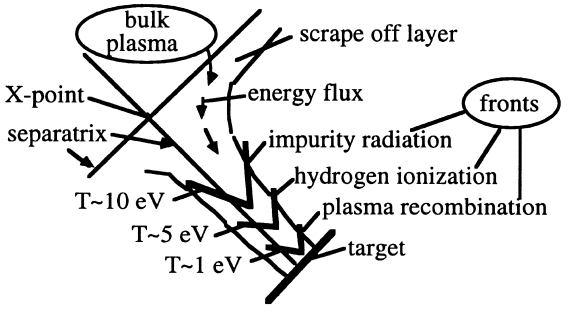

Fig. 1. Schematic view of different regions in a tokamak divertor.

2.1. Instability associated with impurity radiation loss

We will describe impurity radiation loss in the high recycling divertor by a 2D reaction–diffusion equation

$$\partial_y[\kappa_p(T)\partial_y T] + [\kappa_\perp(T)\partial_x T] = R(T), \quad (1)$$

where y and x are the poloidal and radial coordinates ($0 < y < L$), $\kappa_\perp$ is the cross field anomalous heat conduction coefficient, $\kappa_p(T) = (B_p/B)^2\,\kappa_{||}(T)$, $\kappa_{||}(T) \propto T^{5/2}$ is the classical parallel heat conduction coefficient and B_p and B are the strengths of poloidal and total magnetic fields, and $R(T) \equiv \left[(P_{up})^2 \xi_{imp} G_{imp}(T)\right]/T^2$ describes impurity radiation. Here, we assume coronal approximation for the impurity emissivity, $G_{imp}(T)$; fixed impurity fraction, ξ_{imp}; and constant plasma pressure, $P = P_{up}$, along the magnetic field lines. Since $G_{imp}(T)$ is strongly peaked at low temperature we assume that $R(T) > 0$ in a small interval δT_R around the temperature T_R so that $R(T)$ behaves somewhat like a delta function. Since the plasma density in the radiation region is $n_R \approx P_{up}/T_R$, the impurity radiation loss increases with increasing P_{up}.

Consider the one dimensional approximation ($\delta_x = 0$) with heat flux $q_{div} \propto Q_{SOL}$ at the entrance into divertor ($y = L$) and $T_t < T_R$ at the target ($y = 0$) as boundary conditions. The solution of Eq. (1) then only exists for $q_{div}^2] > q_R^2 = 2\int_0^\infty \kappa_p(T)R(T)\mathrm{d}T \propto .P_{up}^2\xi_{imp}$. This sets a constraint $Q_{SOL} > \hat{Q}_{imp}(P_{up}) \propto .P_{up}\sqrt{\xi_{imp}}$. In a sense, this is very similar to a well-known plasma density limit caused by impurity radiation loss from the core (see for example Ref. [6]). The only difference is that here we are dealing with plasma pressure and parallel heat conduction (as a result of parallel plasma transport), while in Ref. [6] it was density and anomalous heat conduction (as a result of cross field plasma transport).

However, due to the coupling of poloidal and radial heat transport (Eq. (1)), cross field anomalous transport is important for impurity radiation loss from the divertor as well. Analysis of Eq. (1) in the 2D case shows that radiation losses can be significantly enhanced in comparison with a 1D treatment due to an increase of the radiation front width caused by cross field anomalous heat conduction even though $\kappa(T) \equiv \kappa_p(T)/\kappa_\perp \gg 1$ [7]. This effect is important when the function $\kappa(T)$ increases with increasing T and the radiation front is V-shaped along the poloidal coordinate. These considerations lead to the estimate for critical value $\hat{Q}_{imp}(P_{up}) \propto q_R\sqrt{\kappa(T_{up})/\kappa(T_R)} \gg q_R$ (where T_{up} is the upstream plasma temperature, $T_{up} \gg T_R$).

2.2. Ionization–recombination instability

Here we present only the main physical reasons for the ionization–recombination instability in the SOL plasmas with some numerical illustrations. Detailed results will be published elsewhere.

Recall that neutral ionization results in energy loss. Therefore, if the neutral flux into a relatively hot ionization region is $\Gamma_{\rm ion}^{(\rm N)}$, then, in steady state, the power $Q_{\rm H}$ must satisfy

$$Q_{\rm H} > E_{\rm ion}\Gamma_{\rm ion}^{(\rm N)}. \quad (2)$$

When $Q_{\rm H}$ drops, $\Gamma_{\rm ion}^{(\rm N)}$ must be reduced to sustain steady-state. However, $\Gamma_{\rm ion}^{(\rm N)}$ is determined by the source of the neutrals and neutral transport through the cold plasma region ("plasma buffer") with characteristic width $\Delta_{\rm b}$, located between neutral source and ionization front (Fig. 2). The temperature in the plasma buffer, $T_{\rm b}$, is low, and few neutrals are ionized there. Neutral transport in this region is determined by neutral-ion collisions and has a diffusive nature. From a fluid description of neutral momentum balance equation (see for example Ref. [8]), we find that the expression for neutral specific flux, $j_{\rm N}$, can be written as

$$j_{\rm N} = -\{2T/[MK_{\rm iN}(2P_{\rm N} + P_{\rm p})]\}\partial_y P_{\rm N}, \quad (3)$$

where $P_{\rm p}$ and $P_{\rm N}$ are the plasma and neutral gas pressures, $K_{\rm iN}$ is the ion-neutral collision rate constant which roughly scales as $K_{\rm iN} \propto \sqrt{T}$ (we assume equal plasma and neutral temperatures). With decreasing energy flux, $Q_{\rm H}$, the temperature and plasma pressure near the neutral source decrease. Decrease of $P_{\rm p}$ can be seen from expression of plasma flux onto the target, $j_{\rm p}$, (notice that from mass conservation we have $j_{\rm N} + j_{\rm p} = 0|j_{\rm p}| \propto (P_{\rm p}/\sqrt{T})_{\rm target}$. Since both $j_{\rm N}$ and $|j_{\rm p}|$ must decrease with decreasing $Q_{\rm H}$ to satisfy inequality Eq. (2), $P_{\rm p}$ should decrease. Meanwhile $P_{\rm N}$ increases in order to sustain plasma-plus-neutral momentum balance along the magnetic field, $P_{\rm N} + P_{\rm p} \leqslant P_{\rm up}$. From Eq. (3) we find that $\Gamma_{\rm ion}^{(\rm N)} \propto j_{\rm N} \propto (P_{\rm p}/\sqrt{T}/\Delta_{\rm b}$. Therefore, to reduce $\Gamma_{\rm ion}^{(\rm N)}$ at $Q_{\rm H} \to 0$, it is necessary to reduce the ratio $\sqrt{T_{\rm b}}/\Delta_{\rm b}$.

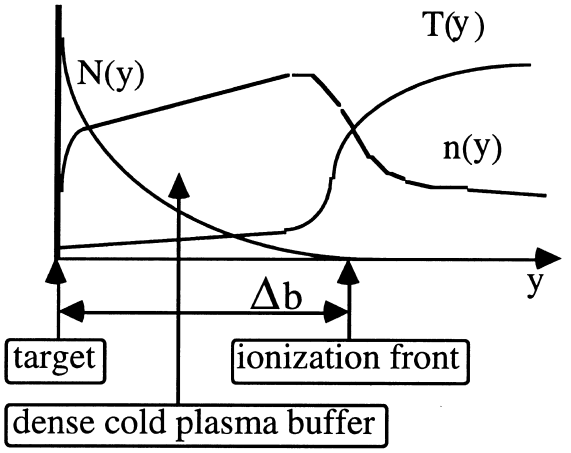

Fig. 2. Plasma temperature, $T(y)$, density, $n(y)$, and neutral gas density, $N(y)$, profiles for the case when plasma neutralizes at the target.

In the case when there is no recombination and the plasma only neutralizes at the target (Fig. 2), $\sqrt{T_{\rm b}}/\Delta_{\rm b}$ can be reduced by decreasing $T_{\rm b}$ or increasing $\Delta_{\rm b}$. However, in practice, volume recombination is not absent. Moreover, the three-body recombination rate strongly increases with decreasing temperature and increasing plasma density. Therefore, trying to reduce $\Gamma_{\rm ion}^{(\rm N)}$ to satisfy energy-balance constraint Eq. (2) at $Q_{\rm H} \to 0$ by lowering $T_{\rm b}$ or increasing $\Delta_{\rm b}$, we face situation where plasma starts to recombine in the plasma buffer itself. As a result, the source of neutrals changes from the target to the buffer region (Fig. 3) and results in both lower $\Delta_{\rm b}$ and higher neutral influx into ionization region. However, higher neutral flux into hot plasma leads to upstream plasma cooling and shift of both ionization and recombination regions further upstream. At the powers $Q_{\rm H}$ below critical, $\hat{Q}_{\rm rec}(P_{\rm up})$, this shift becomes continuos movement of the ionization–recombination fronts to upstream. As a result of the neutral source provided by plasma recombination, the SOL plasma can only be sustained in a steady state condition for $Q_{\rm H} > \hat{Q}_{\rm rec}(P_{\rm up})$. Notice, that this inequality can also be written in the form $P_{\rm up} < \hat{P}_{\rm rec}(Q_{\rm H})$, where $\hat{P}_{\rm rec}(Q_{\rm H})$ is a highest upstream pressure which can be maintained with power $Q_{\rm H}$.

3. Evolution of the fronts in a tokamak divertor

Thus, for $Q_{\rm SOL} < \hat{Q}_{\rm imp}(P_{\rm up})$ and/or $Q_{\rm H} < \hat{Q}_{\rm rec}(P_{\rm up})$, the divertor plasma cannot be sustained in steady-state because of the energy flux deficit into impurity and/or hydrogen radiation fronts which causes the cooling of the plasma in the regions behind these fronts. As a result, plasma from upstream starts to flow into these cold regions and impurity radiation and/or ionization–recombination fronts propagate towards the heat source,

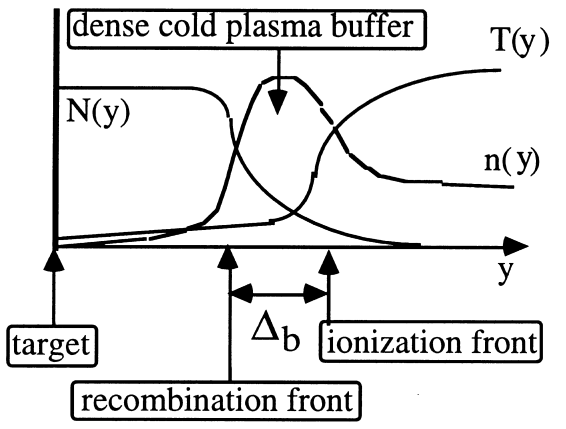

Fig. 3. The same as in Fig. 2 but for the case when plasma recombines volumetrically.

leaving behind a relatively dense, cold, and only partly ionized, plasma with a temperature below the front temperature, T_f. However, if the total number of particles in the SOL is conserved (no fluxes of particles into the SOL either from the core or from puffing systems) then the plasma flow from upstream into recycling region leads to reduction of both upstream plasma pressure P_{up} and, therefore, $\hat{Q}_{imp}(P_{up})$ and $\hat{Q}_{rec}(P_{up})$. As a result a new equilibrium with lower P_{up} can be established.

To find how quickly a new equilibrium, in respond to a substantial change of $\bar{N}_{SOL}$ can be reached, let us estimate the speed V_f of the front propagation along poloidal direction for the case, where the energy flux Q is close to the critical value Q_{crit}. From the energy balance equation, assuming that V_f is sub-sonic, we find

$$\frac{V_f}{C_f} \approx \frac{Q_{crit} - Q}{Q_{crit}} \left(\frac{3}{5} \frac{Q_{crit}}{P_{up} C_f} \right) \equiv \frac{Q_{crit} - Q}{Q_{crit}} \tilde{V}_f, \quad (4)$$

where $C_f = \sqrt{T_f/M}$ is the sound speed at the front temperature. A crude estimate of $\tilde{V}_f$ for the impurity radiation front, $\tilde{V}_f^{imp}$, can be based on the 1D model for $Q_{crit} \equiv \hat{Q}_{imp}(P_{up})$. It gives $\tilde{V}_f^{imp} \sim 1$ for ξ_{imp}, $\sim 10^{-2}$, $\delta T_R \sim T_R \sim 10$ eV, and Gimp $(T_R) \sim 10^{-25}$ W/cm^3. An estimate of the ionization–recombination front velocity gives a similar value.

Thus, V_f is relatively high ($\sim C_f$) even at a low ratio $(Q_{crit} - Q)/Q_{crit}$. Therefore, we can assume that the time scale of establishing a new SOL equilibrium with $Q \approx Q_{crit}$, is shorter than the time scales of the variation of both total number of particles (ions and neutrals) in the SOL, $\bar{N}_{SOL}$, (due to either plasma flow from the core or external particle source) and Q_{SOL} (we assume that ξ_{imp} is fixed). Then, all plasma parameters can be determined from quasi-equilibrium conditions $Q_{SOL} \leqslant \hat{Q}_{imp}(P_{up})$ and $Q_H \leqslant \hat{Q}_{rec}(P_{up})$.

We now compare the predictions of our simplified analytic model with 2D UEDGE [9] simulation results for the variation of the upstream plasma pressure, P_{up}, and density, n_{up}, with $\bar{N}_{SOL}$. All UEDGE runs presented here were performed for a Cartesian slab geometry with total poloidal length of 1 m, target to X-point poloidal length of 0.25 m, total radial width 5 cm (including 1 cm within the core), and 'toroidal' length 1 m which only defines the effective volume. Symmetry boundary conditions are used on the poloidal boundary opposite the target. We conserve total number of particles $\bar{N}_{SOL}$ and fix the power incoming to the system through the core boundary to $Q_{SOL} = 48$ kW. Plasma cross field diffusion coefficient and heat diffusivity are 0.5 and 0.7 m^2/s, respectively, and the ratio of poloidal to total B-field is $B_p/B = 0.06$. We used flux limited parallel heat conduction transport and 1D Navier-Stokes neutrals with radial diffusive transport [10]. More detailed discussion of 2D modeling results will be reported elsewhere.

At low $\bar{N}_{SOL}$ values, when the plasma at the target is hot and neither impurity radiation nor plasma recombination are important, both n_{up} and P_{up} increase with increasing $\bar{N}_{SOL}$. However, the plasma temperature near the target T_t decreases with increasing $\bar{N}_{SOL}$ due to plasma recycling. Therefore, at some value of $\bar{N}_{SOL} = (\bar{N}_{SOL})_{imp}$ we will have $T_t \sim T_R$ and impurity radiation may be important for $\bar{N}_{SOL} = (\bar{N}_{SOL})_{imp}$ at high ξ_{imp}

Consider first the case when impurity radiation loss is small, $Q_{rad}^{(imp)} \ll Q_{SOL}$. Then both n_{up} and P_{up} will continue to increase and T_t will continue to drop with increasing $\bar{N}_{SOL}$ until we reach the point $\bar{N}_{SOL} = (\bar{N}_{SOL})_{rec}$ when $Q_H \approx Q_{SOL} \approx \hat{Q}_{rec}(P_{up})$ and the effects of plasma recombination on energy balance start to be important. Further increase of $\bar{N}_{SOL}$ causes a shift of the ionization–recombination front towards the X-point while keeping $P_{up} \approx \hat{P}_{rec}(Q_H)$. Moreover, since the upstream plasma temperature is insensitive to downstream conditions, being determined mainly by core power input, the constraint imposed on P_{up} by plasma recombination is what limits n_{up}, leading to the inequality $n_{up} \lesssim \hat{n}_{rec}(Q_H)$. We should emphasize that without recombination effects both n_{up} and P_{up} would continue to increase with $\bar{N}_{SOL}$ [11] (assuming that $Q_{rad}^{(imp)}$ stays low). Therefore, our results showing the importance of recombination contradicts to the approach of analytic analysis of Ref. [12], where recombination effects were not considered explicitly.

Comparison with 2D UEDGE results (Fig. 4) shows that with recombination effects turned on, n_{up} increases with increasing $\bar{N}_{SOL}$ for $\bar{N}_{SOL} < (\bar{N}_{SOL})_{rec}$ saturates at $\bar{N}_{SOL} \approx (\bar{N}_{SOL})_{rec}$ and then even decreases with increasing $\bar{N}_{SOL}$ for $\bar{N}_{SOL} > (\bar{N}_{SOL})_{rec}$ (simultaneously, the ionization–recombination front starts to move towards X-point). When the ionization–recombination front reaches about half way to the X-point, n_{up} again increases with increasing $\bar{N}_{SOL}$, first slowly and then rap-

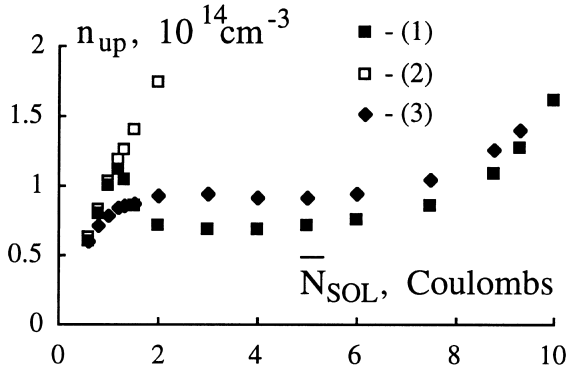

Fig. 4. Dependence of n_{up} on $\bar{N}_{SOL}$ found from 2D UEDGE modeling: (1) with hydrogen recombination, but no impuirites; (2) no hydrogen recombnation, nor impurities; and (3) 0.2% carbon impurity, but no hydorgen recombination.

idly, as the power from the SOL begins to go directly into the ionization–recombination front due to cross field transport. Again, without recombination effects n_{up} always increases with increasing $\bar{N}_{SOL}$.

Next consider the case for $T_t \sim T_R$ when impurity radiation loss is large, $Q_{rad}^{(imp)} \approx Q_{SOL}$ but $Q_{SOL} - Q_{rad}^{(imp)} \gg Q_H$ and recombination effects are not important yet. In this case a further increase of $\bar{N}_{SOL}$ will result either in the saturation of n_{up} and P_{up} or even in their reduction (if, for example, there is a bifurcation of impurity radiation front) to maintain energy balance $\hat{Q}_{imp}(P_{up}) \approx Q_{SOL}$. When $Q_{rad}^{(imp)}$ increases so much that $Q_{SOL} - Q_{rad}^{(imp)}$, $\approx Q_H$ ionization–recombination fronts will also move towards the X-point.

The UEDGE results of the impact of impurity radiation is shown in Fig. 4, where the impurity is modeled in a fixed-fraction approximation with 0.2% carbon, and recombination is turned off. As shown in Fig. 4, the dependence of n_{up} on $\bar{N}_{SOL}$ for impurity radiation only is somewhat similar to that found for case of pure hydrogen plasma when recombination effects are included. However, the local maximum on the dependence of n_{up} on $\bar{N}_{SOL}$ is much less pronounced.

Thus we find that the physical picture of the evolution of the fronts in a tokamak divertor which follows from simplified analytical analysis agrees, in general, with comprehensive 2D modeling.

The inverse dependence of n_{up} on $\bar{N}_{SOL}$ seen in 2D modeling may result in the bifurcation of the SOL plasma parameters due to the SOL–core plasmas coupling. Indeed, if we assume that particle exchange between the core and SOL is due to plasma diffusion and convection, then the core–SOL particle balance equation can be written as

$$\frac{d\bar{N}_{SOL}}{dt} = \hat{D}_s\left[\alpha_{D/V}\bar{n}_{core} - \hat{n}_{up}(\bar{N}_{SOL})\right], \quad (5)$$

where $\bar{n}_{core}$ is the averaged plasma density in the core, the function $\hat{n}_{up}(\bar{N}_{SOL})$ is determined from the SOL equilibrium, and $\hat{D}_s$ and $\alpha_{D/V}$ describe plasma flow through core-SOL boundary due to diffusion and convection. Usually the particle content in the core is large, thus both $\bar{N}_{SOL}$ and $\bar{n}_{core} \approx$ constant. From Eq. (5) it can be seen that the core-SOL equilibrium, $\hat{n}_{up}(\bar{N}_{SOL}) = \alpha_{D/V}\bar{n}_{core}$, becomes unstable when $\hat{n}_{up}(\bar{N}_{SOL})$ decreases with increasing $\bar{N}_{SOL}$. In this case $\bar{N}_{SOL}$ and, therefore, the fronts can experience the 'jump' towards the X-point.

4. Comparison with experimental observations

We compare the results of our theoretical analysis of the evolution of the fronts with experimental observations from Alcator C-Mod tokamak based on bolometric, spectroscopic (D_α) and probe measurements [1,13]. We analyze a well-documented shot (ohmic discharge with toroidal magnetic field strength 5 T and plasma current 0.8 MA), where the detached divertor regime was achieved by intense gas puffing (see also Refs. [14,15]). Fig. 5 shows the time evolution of the core plasma density, $\bar{n}_{core}$; power to the SOL, Q_{SOL}; plasma flux on the outer target (below the "nose") from the target probe measurements, Φ_{out}; D_α, D_α^{out} and bolometric, Q_{bol}^{out}, signals from the chords viewing the outer divertor leg (see straight lines in Figs. 6 and 7); and neutral gas pressure in the divertor, P_g. In the same figure the upstream plasma density n_{up} and electron temperature, T_{up}, are shown for three time slices at a distance of 1 mm from the separatrix (at midplane projection), as measured by a reciprocating probe, The tomographic reconstruction of bolometric and # intensity measurements are shown in Figs. 6 and 7, respectively.

From the data, Q_{bol}^{out} starts to increase at 0.6 s and a radiation front starts to move towards the X-point (see Fig. 6), reaching it at ~0.8 s. The D_α^{out} signal starts to increase strongly (see Fig. 5), and the D_α-front starts to propagates to the X-point (see Fig. 7) at 0.8 s. Knowing from a previous study [16] that the strong increase in D_α is associated with plasma recombination, we expect and observe (Fig. 5) a significant reduction of Γ_{out} which starts at about 0.8 s. From spectroscopic data [13] we can expect the plasma density in the recombination region, n_{rec}, to be of the order of 10^{15} cm^{-3}. Notice, that from 0.6 to 1 s Q_{SOL}, n_{up}, and T_{up}, only vary within 10–20% (with the trend to be lower after detachment occurs), while P_g continuously rises from 4 to about 40

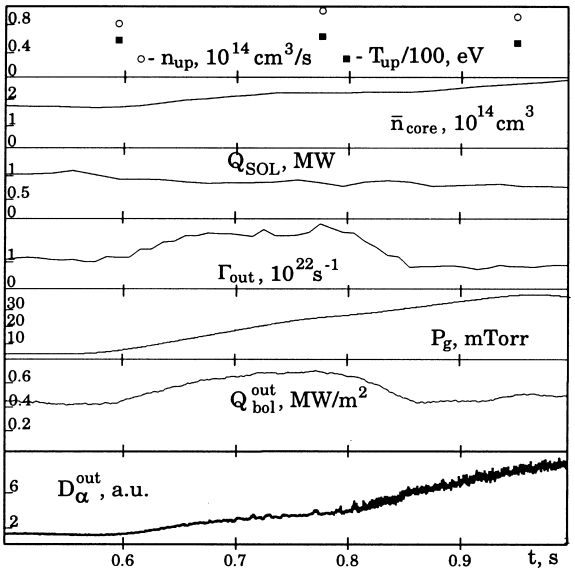

Fig. 5. Time variation of the plasma parameters from Alcator C-Mod discharge.

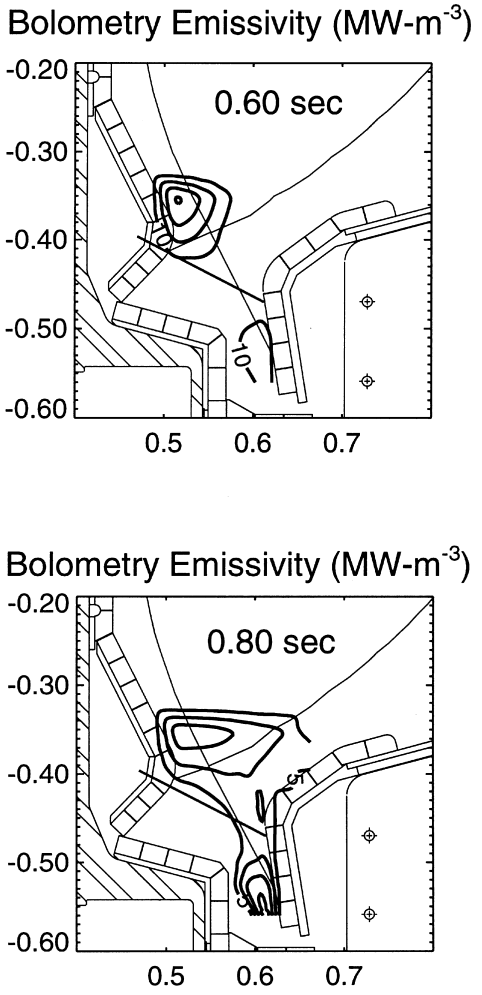

Fig. 6. The tomographic reconstruction of bolometric measurements; solid straight line shows $Q_{\rm bol}^{\rm out}$ chord from Fig. 5.

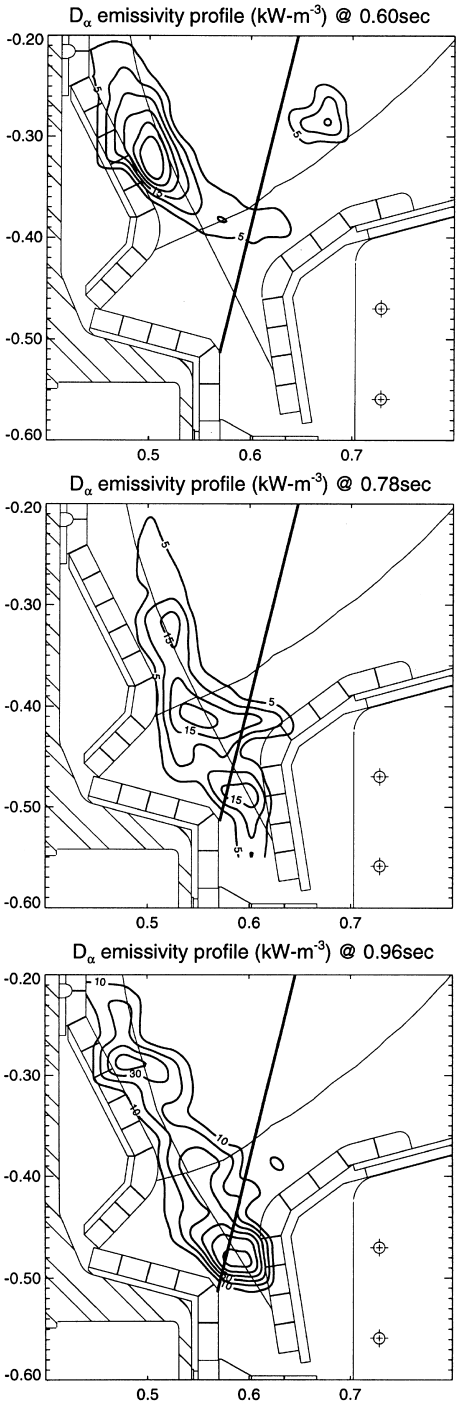

Fig. 7. The tomographic reconstruction of D_z measurements; solid straight line shows D_z chord from Fig. 5.

mTorr. The increase of $P_{\rm g}$ and the high plasma density in the recombination region, suggests that $\bar{N}_{\rm SOL}$ significantly increases during the transition from attached to detached regime. A crude but conservative estimate of the variation of $\bar{N}_{\rm SOL}$ (without taking into account radial broadening of plasma density in the detached regime) based on $n_{\rm up} \sim 10^{14}$ cm^{-3}, $n_{\rm rec} \sim 10^{15}$ cm^{-3}, poloidal length of the cold plasma region $\sim$5 cm, and $P_{\rm g} \sim 40$ mTorr (in detached regime) shows that $\bar{N}_{\rm SOL}$ roughly doubles between 0.6 and 1 s while upstream plasma parameters remain almost the same. In other words, in agreement with theory/modeling results we find that, for fixed power into SOL and increasing $\bar{N}_{\rm SOL}$, upstream plasma parameters stay almost constant while first the impurity radiation front and then the ionization–recombination front both propagate towards X-point. In general, Alcator C-Mod data confirm theoretical picture of front propagation on a qualitative level. More work is needed to sort out the effects of inner and outer divertor interactions.

5. Conclusions

Analytical analysis and numerical modeling show that impurity radiation and plasma recombination effects play a crucial role in the evolution of detached plasma parameters. These effects alter the energy balance in tokamak SOL and result in the saturation (or even reduction) of the upstream plasma density and temperature with increasing total number of particles (ions and neutrals) in the SOL. They cause both the impurity radiation and ionization–recombination fronts to propagate towards the X-point. These conclusions are supported by experimental data from the Alcator C-Mod tokamak. Of course, more work is needed for detailed quantitative comparison of theoretical and experimental results.

Acknowledgements

Work performed for USDOE under contracts DE-FG02-91-ER-54109 at MIT and W-7405-ENG-48 at LLNL.

References

[1] J.A. Goetz et al., Phys. Plasmas 3 (1996) 1908.
[2] M.E. Fenstermacher et al., J. Nucl. Mater. 241–243 (1997) 666.
[3] T.D. Rognlien et al., 24th EPS Conference, Berchtesgaden, Germany, P3.071, 1997.
[4] A.S. Kukushkin et al., 16th IAEA Fusion Energy Conference, Montreal, 1996.
[5] D.P. Coster et al., 24th EPS Conference, Berchtesgaden, Germany, P4.1437, 1997.
[6] P.H. Rebut, B.J. Green, 11th IAEA Conference, Berchtesgaden, Germany, 1976; International Atomic Energy Agency, vol. 2, Vienna, Italy, 1977, p. 3.
[7] S.I. Krasheninnikov, Phys. Plasmas 4 (1997) 3741.
[8] P. Helander, S.I. Krasheninnikov, P.J. Catto, Phys. Plasmas 1 (1994) 3174.
[9] T.D. Rognlien et al., J. Nucl. Mater. 196–198 (1992) 347.
[10] F. Wising et al., Contrib. Plasma Phys. 36 (1996) 132.
[11] S.I. Krasheninnikov et al., Nucl. Fusion 27 (1987) 1805.
[12] K. Borrass, R. Schneider, R. Farengo, Nucl. Fusion 37 (1997) 523.
[13] B. LaBombard et al., Phys. Plasmas 2 (1995) 2242.
[14] B. Lipschultz et al., these Proceedings.
[15] J.L. Terry et al., these Proceedings.
[16] J.L. Terry, et al., Phys. Plasmas 5 (1998) 1759.